Observations of Velocity Divergence in Shelikof Strait, Alaska

R.K. Reed and P.J. Stabeno

National Oceanic and Atmospheric Administration
Pacific Marine Environmental Laboratory
Seattle, Washington 98115

Contribution No. 1275 from NOAA's Pacific Marine Environmental Laboratory

ABSTRACT — Direct observations of horizontal velocity divergence and relative vorticity were made in Shelikof Strait, Alaska during May 1990 with Loran-C buoys and satellite-tracked drifters. These kinematic properties typically had values of $2 \times 10^{-5}\ s^{-1}$. The horizontal divergence was a clearly defined, mesoscale process not apparently affected by turbulent diffusion. The divergence also appeared to be linked to the rise and fall of the pycnocline driven by an internal, semidaily tide. The data suggested that the net divergence over several days was quite small; thus larval concentration models can ignore this effect.

INTRODUCTION

Since 1984 the Pacific Marine Environmental Laboratory has participated in the Fisheries Oceanography Coordinated Investigations (FOCI) in Shelikof Strait, Alaska (Fig. 1). The goal of FOCI is to gain understanding of the biotic and abiotic environments and their effects on recruitment of pollock, which spawn each spring in a small area of the central strait. The resulting larvae rise into the upper ocean and are affected by currents (advection), turbulent diffusion, and the divergence of velocity. Although velocity divergence can be ignored for many oceanic processes, the swimming behavior of larvae tends to cancel the vertical component of divergence, and the larvae are thus subject to being spread or concentrated by the *horizontal* divergence or convergence (OLSON and BACKUS, 1985). Consequently, we were interested in measuring the horizontal divergence of velocity for use in a larval concentration model that is being developed for this region.

Various methods exist for deriving estimates of horizontal divergence; the rise or fall of isotherms or isopycnals may be monitored at a site, and the net vectors from Eulerian current measurements can be used for crude estimates of the divergence in the velocity field. On the other hand, a water parcel may be "tagged" with floating devices to directly measure changes in area and thus horizontal velocity divergence. This direct, Lagrangian method was used successfully by CHEW and BERBERIAN (1971) and REED (1971). MOLINARI and KIRWAN (1975) presented further observations, and they also discussed aspects of the kinematic properties and of turbulent diffusion. These studies all examined data from relatively swift flows; the horizontal divergence and relative vorticity were typically 10^{-5} s^{-1}. Over areas of a few to ~20 km^2, the kinematic properties were deterministic and appeared to be little influenced by turbulent diffusion.

With the advent of satellite-tracked drifting buoys, the emphasis has been on measuring large-scale ocean flows rather than mesoscale kinematic properties. Recently, however, PADUAN and NIILER (1990) derived horizontal divergence and relative vorticity from satellite-tracked drifter data off California. In this study, we use data from both satellite-tracked drifters and Loran-C buoys in the Shelikof Strait region.

DATA AND METHODS

The satellite-tracked drifting buoys used here were manufactured by Seimac Limited. They employed "tristar" drogues, which were centered at 40 m depth. At this latitude, we typically received 15–18 fixes per day. REED and STABENO (1990) reported a test performed on this type of drifter, near this latitude, that indicated the standard error of an individual fix was 0.18 km.

Two different types of Loran-C buoys were used. Those manufactured by Candel Industries (buoy numbers 1, 2, and 3 below) used a "light-bulb" shaped surface buoy, which housed an antenna, flasher, and data logger that stored the Loran rates. A 10 m long "holey sock" drogue was centered at 40 m. CRAWFORD (1988) reported a test with this type system that indicated a standard error of position of 24 m, which is appreciably better than the value above for satellite-tracked drifters. The other type of Loran-C buoy was manufactured by Seimac Limited (buoy numbers A and B below). It had a surface float, made from plastic pipe, with a "tristar" drogue centered at 40 m. Position data from these buoys were received and logged aboard ship, with a reception range of ~1 km.

Various methods of using Lagrangian data for computation of kinematic properties were discussed by MOLINARI and KIRWAN (1975). (Since we are concerned with area change and its effects on larvae, the deformation terms have been ignored.) Two simple methods, which allow comparison of estimates, were used here. In principle, the horizontal divergence of velocity may be estimated from

$$div_h \vec{V} = \frac{1}{A}\frac{dA}{dt}, \tag{1}$$

where A is the area determined from a drifter triad, and t is time. If friction is assumed negligible and since the Coriolis parameter is nearly constant, we have a simplified form of the vorticity equation

$$div_h \vec{V} = -\frac{1}{(\zeta + f)}\frac{d\zeta}{dt}, \tag{2}$$

where ζ is the vertical component of relative vorticity (twice the angular rotation of a line segment), and f is the Coriolis parameter. With the further assumption of nearly uniform angular acceleration, (2) can be used to also estimate horizontal divergence and verify the results from (1).

RESULTS

Horizontal divergence estimates from the Loran-C buoys are presented first. As noted above, this system has smaller position errors than the satellite-tracked drifters. A much larger data record is available from the drifters, however, and these results are also examined.

Loran-C buoys

Data from this system were taken during two periods of ~24 hours each. Complete data from three or more buoys, however, were obtained during only two relatively brief periods: 19 May, 0625–1025 and 22 May, 1020–1550. During 19 May, three Loran-C buoys were near the three satellite-tracked buoys, and both sets of buoys were in a well-developed, anticyclonic eddy with a radius of ~10 km. During 22 May, four Loran-C buoys were tracked; they were ~50 km southwest of the satellite-tracked drifters and the eddy. From these four buoys, only two triads were useable because the other possible triads were essentially straight lines.

Figure 2 shows the area of the buoy triad 123 during 19 May, along with the angular orientation of the three line segments. Results of the calculations from these data are given in Table 1. The horizontal divergence of velocity calculated from the area change was 3×10^{-5} s^{-1}. The positive divergence was properly accompanied by clockwise rotation, but two of the three estimates from (2) were appreciably larger than those from area change (Table 1). The excessive rotation in some of the results is presumably related to the rotation of the eddy (~4° hr^{-1}); removal of this eddy rotation would improve agreement for the larger estimates.

Figure 3 shows area plots of the two triads during 22 May, plus angular orientation of the line segments. Estimates of divergence (Table 1) from areas were 2–3×10^{-5} s^{-1}; those from rotation were all 2×10^{-5} s^{-1}, except for the line segment BA which initially rotated counterclockwise and then clockwise. These triads are well south of the eddy, and there is good agreement between the two triads (AB2 and AB3) and for estimates based on areas and rotation. Thus the horizontal divergence appears to be a deterministic process affecting this "tagged" water parcel. The relative vorticity accompanying the divergence was ~2×10^{-5} s^{-1}.

Satellite-tracked drifters

Three satellite-tracked buoys (13, 26, and 35) were deployed on 11 May near the center of a pollock larval patch. It was apparent within a few days that the drifters were in an anticyclonic eddy, but one buoy transmitted only sporadically during the first several days. During 19–28 May, however, data quality was good, and the area formed by the drifters remained relatively constant. The drifters clearly had left the eddy by 1 June.

Figure 4 shows a time series of areas formed by the three drifters during 19–28 May. The dashed lines indicate the time of predicted flood (westward) tidal current at Unga Strait, Shumagin Islands (U.S. DEPARTMENT OF COMMERCE, 1989). In 9 of the 14 cases, flood current occurred during times when the area was increasing. Divergence from the area change of the drifters was typically $1\text{–}5 \times 10^{-5}\ s^{-1}$. Thus there seems to be no major difference in the results from the Loran-C buoys and satellite-tracked drifters, even though the former had generally smaller areas (Figs. 2 and 3) than the latter (Fig. 4).

DISCUSSION

The Loran-C buoy data indicated that horizontal velocity divergence was accompanied by clockwise rotation of line segments as expected. Except when rotation was influenced by the mesoscale eddy, estimates of divergence by (1) and (2) were comparable. The magnitude of horizontal divergence (and relative vorticity) was $2\text{–}3 \times 10^{-5}\ s^{-1}$, which is similar to values reported by CHEW and BERBERIAN (1971), REED (1971), and MOLINARI and KIRWAN (1975). These references, however, reported observations from swift boundary flows with speeds typically two–three times the net flows here. In Shelikof Strait, horizontal divergence occurred as a clearly defined process that was not obviously affected by turbulent diffusion.

As shown in Fig. 4 and noted above, divergence was often accompanied by flood tidal currents. Divergence measured by the Loran-C buoys also occurred during flood currents (0937 and 1204 on 19 and 22 May, respectively). In addition, the observations of CHEW and BERBERIAN (1971), and especially REED (1971), seemed to contain a tidal modulation. A spectral plot of the areas from the satellite drifters showed a well-defined peak (above the 95% significance level) at the semidaily tidal frequency. Shelikof Strait has predominantly alternating, semidaily tidal currents (ISAJI and SPAULDING, 1987), which are somewhat weaker inshore, near the Alaska Peninsula (Fig. 1), than offshore in deeper water. Recent FOCI current observations support this structure; the shear vorticity is of the proper sign during flood currents and horizontal divergence, but the shear does not extend offshore as far as the drifter data. Another plausible mechanism for generating alternating positive and negative horizontal divergence would be through the rise and fall of the pycnocline driven by an internal tide. Figure 5 shows spectral plots of the salinity, which largely controls density in this region, at stations 15–18 (Fig. 1), which is near the location of the satellite-tracked drifter and Loran-C buoy data. At each station there was a well-developed semidaily spectral peak in the pycnocline; above and below, however, the energy density at this frequency was generally reduced. Thus we infer that westward (flood) tidal currents were accompanied by a rising pycnocline and horizontal divergence.

A major objective of this work was to ascertain typical or net horizontal divergence, over the region transited by the pollock larval plumes, for use in a larval concentration model of Shelikof Strait. The drifter data here were within the region where larval patches commonly occur. The data in Fig. 4 showed several alternating zones of positive and negative divergence; except for short-term changes, however, there was little net change in area over this ten-day period. This suggests that horizontal divergence of velocity can be ignored in larval concentration models here.

Acknowledgements — This is a contribution to the Fisheries Oceanography Coordinated Investigations (FOCI-0133) of NOAA. We thank the officers and crew of the NOAA ship *Miller Freeman*; we also appreciate the efforts of C. DeWitt, D. Dougherty, S. Hinckley, D. Kachel, W. Parker, and J. Schumacher. Contribution No. 1275 from NOAA/Pacific Marine Environmental Laboratory.

REFERENCES

CHEW F. and G.A. BERBERIAN (1971) A determination of horizontal divergence in the Gulf Stream off Cape Lookout. *Journal of Physical Oceanography, 1,* 39–44.

CRAWFORD W.R. (1988) The use of Loran-C drifters to locate eddies on the continental shelf. *Journal of Atmospheric and Oceanic Technology, 5,* 671–676.

ISAJI T. and M.L. SPAULDING (1987) A numerical model of the M_2 and K_1 tide in the northwestern Gulf of Alaska. *Journal of Physical Oceanography, 17,* 698–704.

MOLINARI R. and A.D. KIRWAN, JR. (1975) Calculations of differential kinematic properties from Lagrangian observations in the western Caribbean Sea. *Journal of Physical Oceanography, 5,* 483–491.

OLSON D.B. and R.H. BACKUS (1985) The concentrating of organisms at fronts: A cold-water fish and a warm-core Gulf Stream ring. *Journal of Marine Research, 43,* 113–137.

PADUAN J.D. and P.P. NIILER (1990) A Lagrangian description of motion in northern California coastal transition filaments. *Journal of Geophysical Research, 95,* 18,095–18,109.

REED R.K. (1971) An observation of divergence in the Alaskan Stream. *Journal of Physical Oceanography, 1,* 282–283.

REED R.K. and P.J. STABENO (1990) Flow trajectories in the Bering Sea: evidence for chaos. *Geophysical Research Letters, 17,* 2141–2144.

U.S. DEPARTMENT OF COMMERCE (1989) Tidal Current Tables, Pacific Coast of North America and Asia. U.S. Government Printing Office, 287 pp.

Table 1. Estimates of the horizontal divergence of velocity from area change ($\frac{1}{A}\frac{dA}{dt}$) and from the rotation of line segments ($-\frac{1}{\zeta + f}\frac{d\zeta}{dt}$), 19 May and 22 May 1990.

Date/Time	Triangle	$\frac{1}{A}\frac{dA}{dt}$ (10^{-5} s^{-1})	$-\frac{1}{\zeta + f}\frac{d\zeta}{dt}$ (10^{-5} s^{-1})		
19 May 90/0625–1025	123	3.4	16.4	12.2	3.4
22 May 90/1020–1550	AB2	2.4	1.6	1.7	—
	AB3	2.7	1.7	1.7	—

LIST OF FIGURES

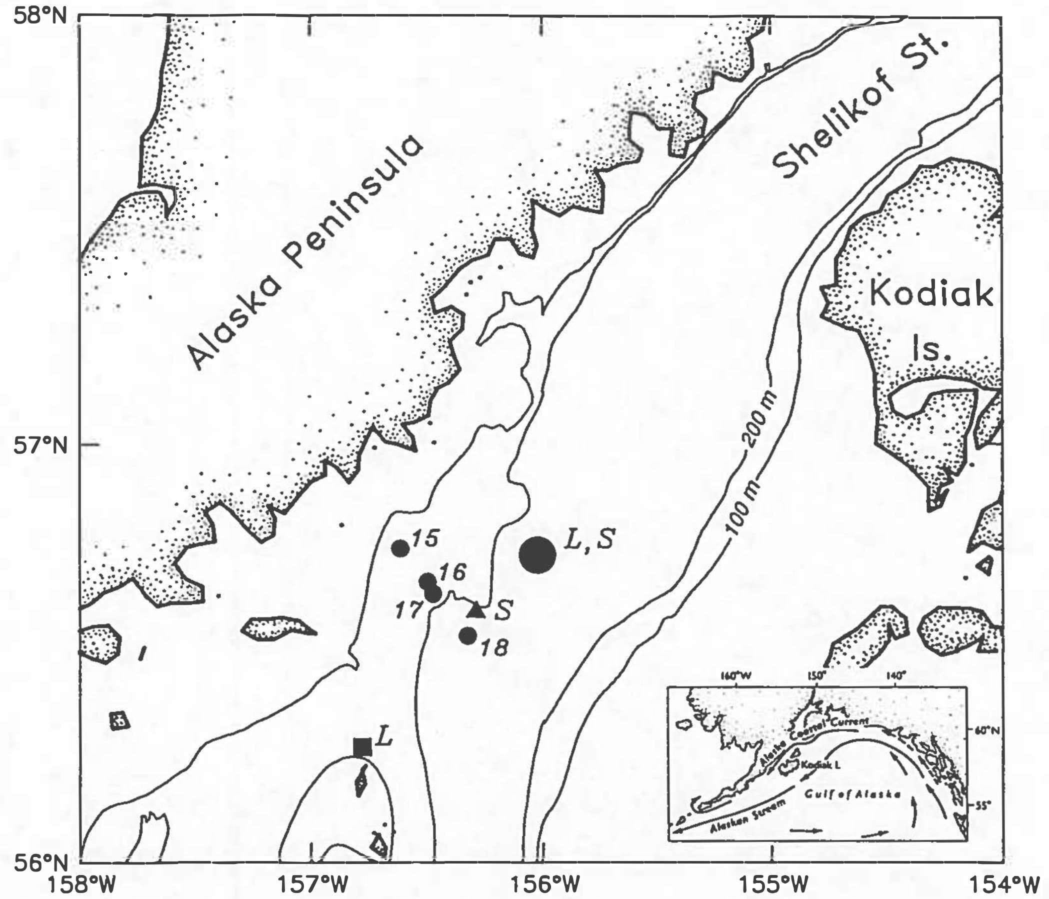
58°N
57°N
56°N
158°W
157°W
156°W
155°W
154°W
Alaska Peninsula
Shelikof St.
Kodiak Is.
200 m
100 m
L, S
15
16
17
S
18
L
160°W
150°
140°
60°N
55°
Alaska Coastal Current
Kodiak I.
Gulf of Alaska
Alaskan Stream

Fig. 1

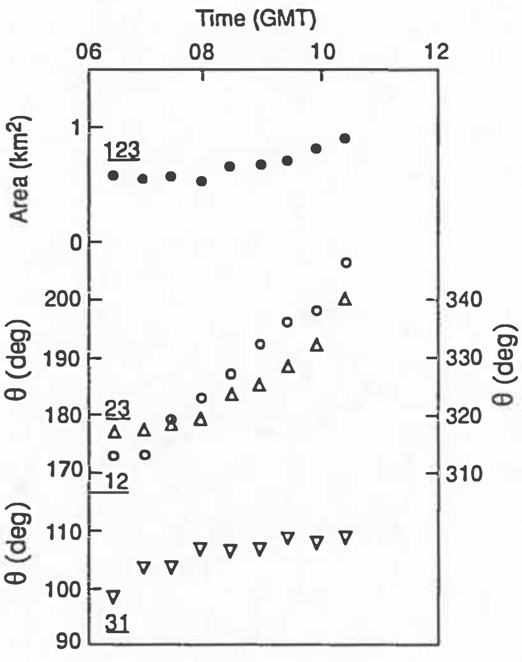
Time (GMT)
06
08
10
12
Area (km^2)
1
0
123
θ (deg)
200
190
180
170
23
12
340
330
320
310
θ (deg)
θ (deg)
110
100
90
31

Fig. 2

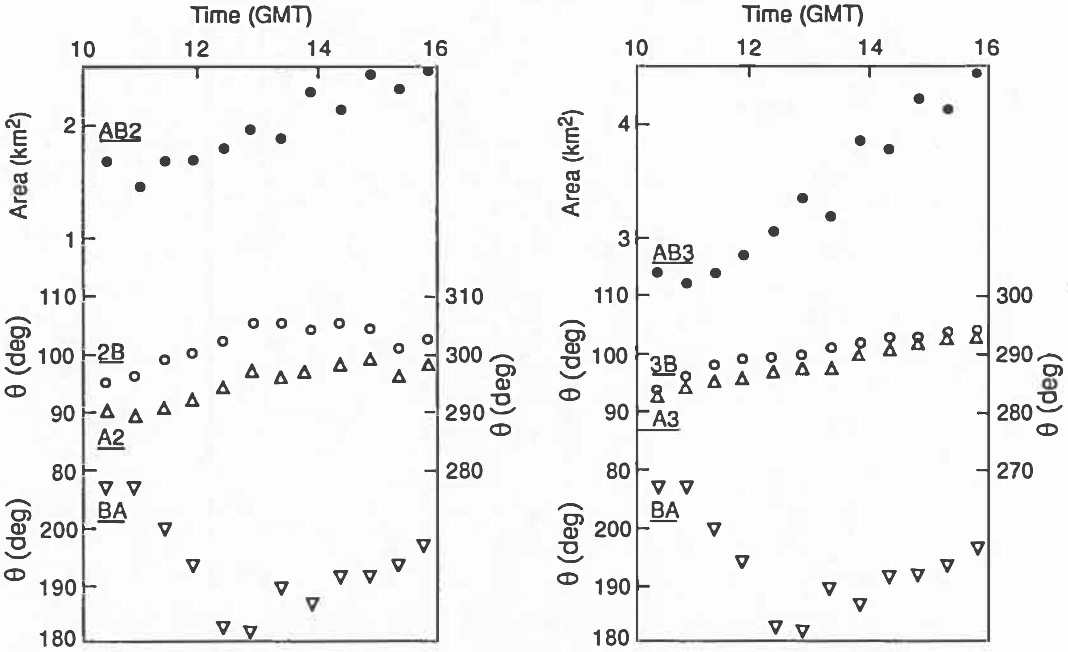
Time (GMT)
10
12
14
16
Area (km^2)
2
1
AB2
110
100
90
80
200
190
180
θ (deg)
2B
A2
BA
310
300
290
280
θ (deg)
Time (GMT)
10
12
14
16
Area (km^2)
4
3
AB3
110
100
90
80
200
190
180
θ (deg)
3B
A3
BA
300
290
280
270
θ (deg)

Fig. 3

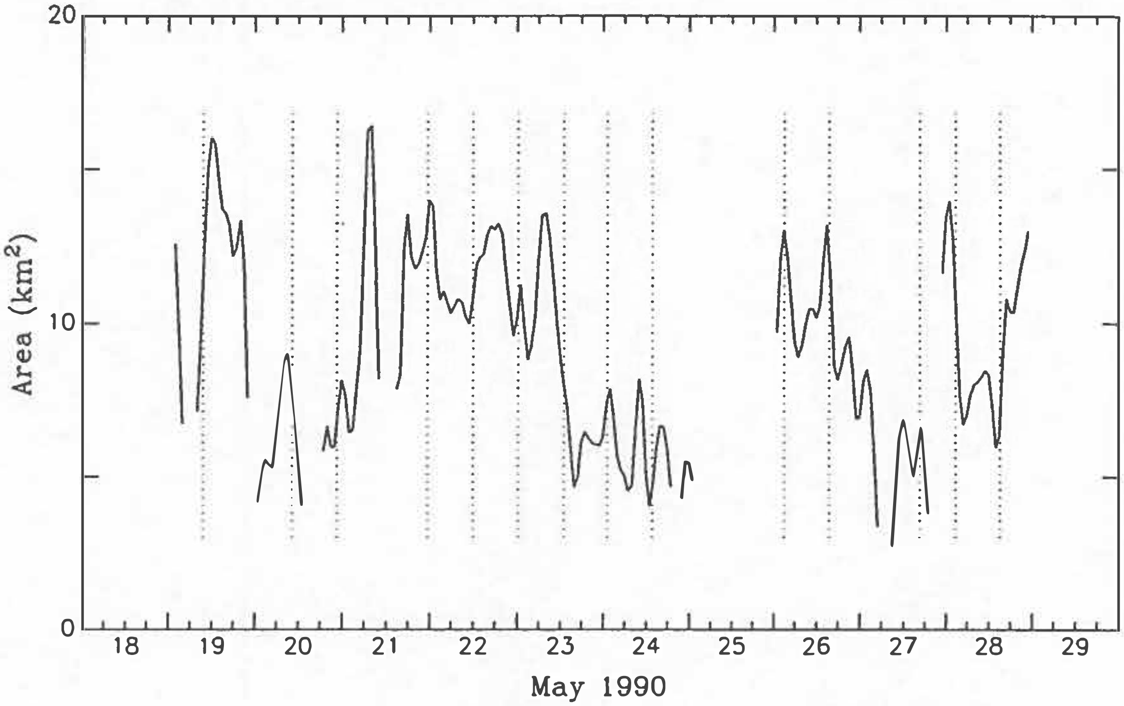

Fig. 4

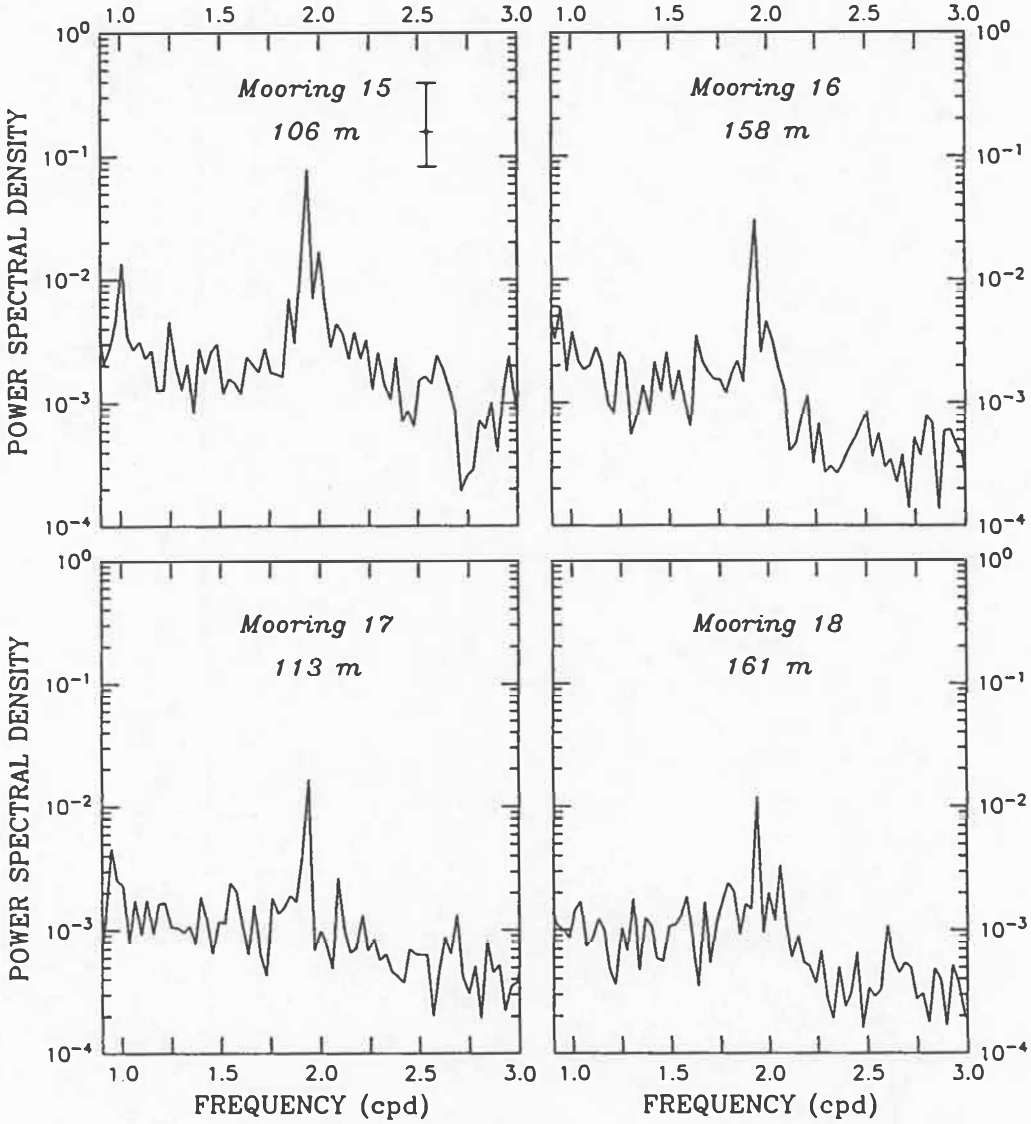

Mooring 15
106 m
Mooring 16
158 m
Mooring 17
113 m
Mooring 18
161 m
POWER SPECTRAL DENSITY
FREQUENCY (cpd)
1.0
1.5
2.0
2.5
3.0
10^0
10^{-1}
10^{-2}
10^{-3}
10^{-4}

Fig. 5